Analysis of Fracture Morphology in Hydrogen Embrittlement for Cr-Mo Steel†

Toshio ENJO*, Toshio KURODA** and Noriyuki MITSUI***

Abstract

An investigation has been made into the analysis of the fracture morphology of hydrogen embrittlement for a quenched and tempered Cr-Mo steel. The Cr-Mo steel showed the tempered martensite embrittement by 300°C tempering treatment.

The susceptibility to hydrogen embrittlement was highest for the as-equenched specimen, and decreased with increasing tempering temperature. The percentage of intergranular fracture in the fractured surface was highest for the specimen tempered at 300°C.

The fracture morphology of tempered martensite embrittlement was intergranular fracture with flat surface, but the morphology of hydrogen embrittlement was intergranular fracture with tear ridges on the surface. The characteristic morphology of hydrogen embrittlement was quasi-cleavage fracture due to hydrogen (QC_{HE}), which had the same small facet size as martensite lath morphology, with secondary cracks along the martensite lath. This fracture morphology was the same as that of hydrogen embrittlement of HT80 steel previously indicated.

KEY WORDS: (Cr-Mo Steel) (Tempered Martensite Embrittlement) (Hydrogen Embrittlement) (Fractography)

1. Introduction

A Cr-Mo steel contained 0.35% carbons takes place cracks due to quench from austenitization temperature, cold weld cracking, and delayed failure under the corrosion environment such as hydrogen respectively. However, the fracture morphology of hydrogen embrittlement has not been characterized yet.

In the case of the high strength steel (HT80)[1) 2)], it is made clear that the fracture morphology of hydrogen embrittlement is different from that of cleavage fracture occured at low temperature embrittlement, that is, their fracture facet size is smaller than that of the cleavage fracture, and is corresponded to the morphology distribution of the martensite laths. The other way, on the view point of the crystallography, the cleavage fracture of HT80 steel takes place along { 100 } plane, but the hydrogen embrittlement fracture takes place along the { 110 } plane. In the case of delayed cracking of Cr-Mo steel, the relation between 500°F embrittlement, namely tempered martensite embrittlement and characteristics of delayed cracking has been reported[3) 4)]. However, the fracture morphology showed the intergranular fracture only, and has not been analized exactly. And the morphology of transgranular fracture due to hydrogen embrittlement has not been observed.

Then, an investigation has been made of, based on the fractography, the relation between tempered martensite embrittlement and hydrogen embrittlement, and then characteristic fracture morphologies of hydrogen embrittlement were discovered using fractography.

2. Experimental Procedures

The material used in the present investigation is Cr-Mo steel for the mechanical structure, namely SCM3 in Japan industrial standard (JIS). Their chemical compositions are shown in **Table 1**. A material was received as 16 mm hot-rolled plate. The block samples were machined from the plate, with the long aixs of each sample parallel to the

Table 1 Chemical compositions of material used (Wt%).

C	Si	Mn	P	S	Ni	Cr	Mo	Cu	Sol.Al
0.36	0.20	0.82	0.013	0.007	0.04	1.10	0.16	0.03	0.038

† Received on October 31, 1983
* Professor
** Research Instructor
*** Graduate Student

Transactions of JWRI is published by Welding Research Institute of Osaka University, Ibaraki, Osaka 567, Japan

rolling direction.

The heat treatments for the samples were carried out in argon using a high frequency induction heating equipment, that is, the samples were heated at 850°C to 1350°C for 15 seconds respectively, silicone-oil quenched, and then the subzero treatments performed. Tempered treatments were made using the electric furnance, namely, the specimens were heated at each temperature of 150°C to 600°C respectively for 1.5 hrs., and then water-quenched.

After the treatments, the specimens were exactly cut from the bulk samples. The tensile specimen had 6 mm gage diameter and 40 mm gage length, and Charpy-impact specimens (JIS No.4) were also used. The tensile test and impact test were performed respectively. For the hydrogenation, the specimens were cathodically charged at the current density of 10 mA/cm^2 for 2 hrs in the 5% sulphuric acid solution poisoned with yellow phosphorus and CS_2 as hasten material. No irreversible hydrogen charging damage, such as blistering or internal cracking, was observed metallographically. After the hydrogenation to the specimen, the specimens were pulled out at the cross head speed of 1 mm/min using Instron type machine.

The fracture surfaces obtained were observed exactly using scanning electron microscope. Each fractured specimen was observed about 40 fields of view on the fracture surface, and the percentages of intergranular fracture on the fracture surface observed were evaluated by point counting method using 100 point grids. The microstructures were evaluated by the etchant, namely, at first, prior austenite grain boundaries were evaluated by the piclic acid solution, then the microstructures within the grain were evaluated by 5% Nital.

3. Results and Discussion

3.1 Characteristics of tempered martensite embrittlement

Figure 1 shows the relation between energy transition temperatures ($_vT_{rE}$) and tempering temperature by Charpy impact test. In the case of the specimen austenitized at 850°C, the prior austenite grain size was 10 μm, in the case of 1200°C, the size was 120 μm. The tensile strength decreased with increasing the tempering temperature, but the energy transition temperature suddenly increased above 150°C of tempering temperature. As the tempering temperature is at 300°C, the transition temperature shows maximum value, and then decreases with increasing tempering temperature. The generation of the peak seems to be due to the 500°F embrittlement, namely tempered martensite embrittlement[3)5)6)].

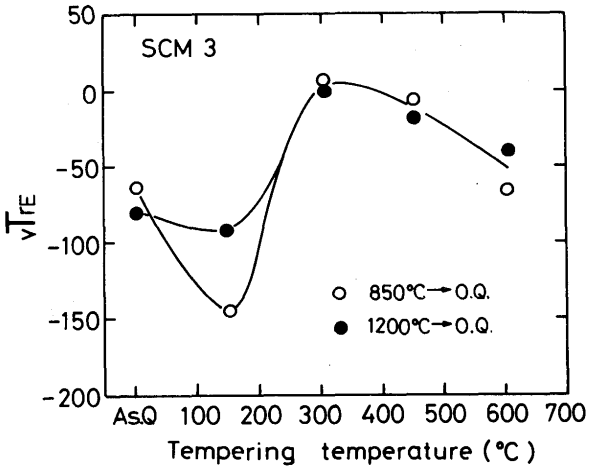

Fig. 1 Relation between energy transition temperature and tempering temperature.

Figure 2 shows the relation between V-notched Charpy impact value (CVN) and tempering temperature. The energy shows minimum value at 300°C of tempering temperature, and it means that the tempered martensite embrittlement takes place at the temperature. About the specimen, the relation between intergranular fracture percentage and the tempering temperature is shown in **Fig. 3**. In the case of the specimen austenitized at 850°C, the intergranular fracture percentage shows about 30% for the tempering temperature at 300°C. However, the intergranular fracture hardly occur for the other tempering temperature. The other way, for the specimen austenitized at 1200°C, as-quenched specimen and specimen tempered at 600°C hardly cause the intergranular fractures. However, the percentage of intergranular fracture is high for the other tempering temperature. Now, the specimens showed the dimple-pattern fractures at the area

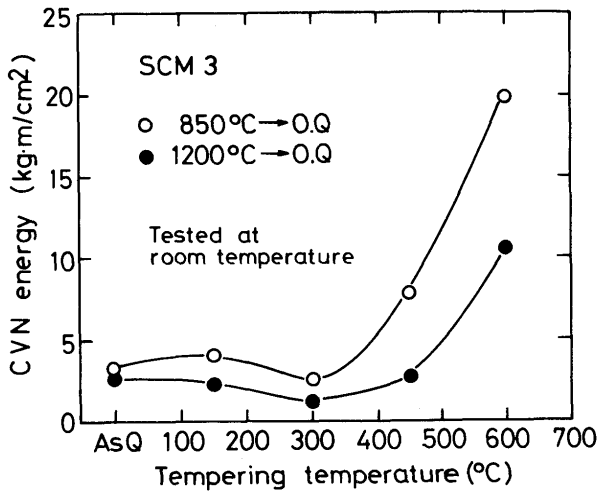

Fig. 2 Relation between Charpy-V-notched (CVN) energy and tempering temperature.

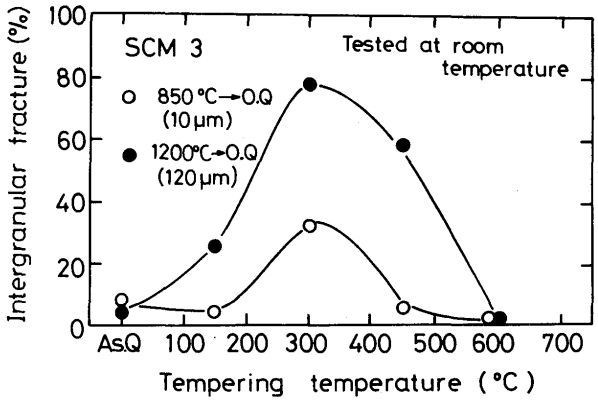

Fig. 3 Relation between percentage of intergranular fracture and tempering temperature.

except the intergranular fracture for every specimens used.

For the specimen tempered at 300°C, among of Charpy impact energy, intergranular fracture percentage and prior austenite grain size are shown in **Fig. 4**. Charpy impact value decreases with increasing the grain size, and the intergranular fracture percentage reversly correspond to the increase. The impact value corresponds to the fracture percentage up to 40% of intergranular fracture. Above the fracture percentage, the impact value hardly change with increasing the intergranular fracture percentage.

Figure 5 indicates the relation between the morphology of intergranular fracture and austenitization temperature for the specimen tempered at 300°C. In the case of the specimen austenitized at 850°C, the morphology of inter-

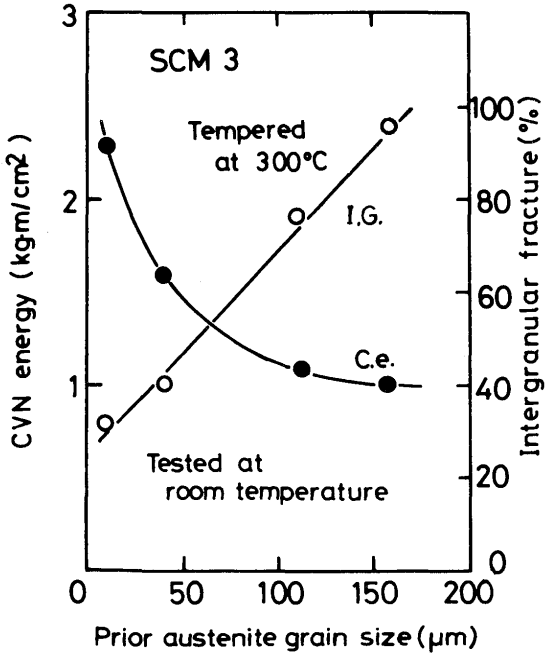

Fig. 4 Relation between CVN energy, percentage of intergranular fracture and prior austenite grain size.

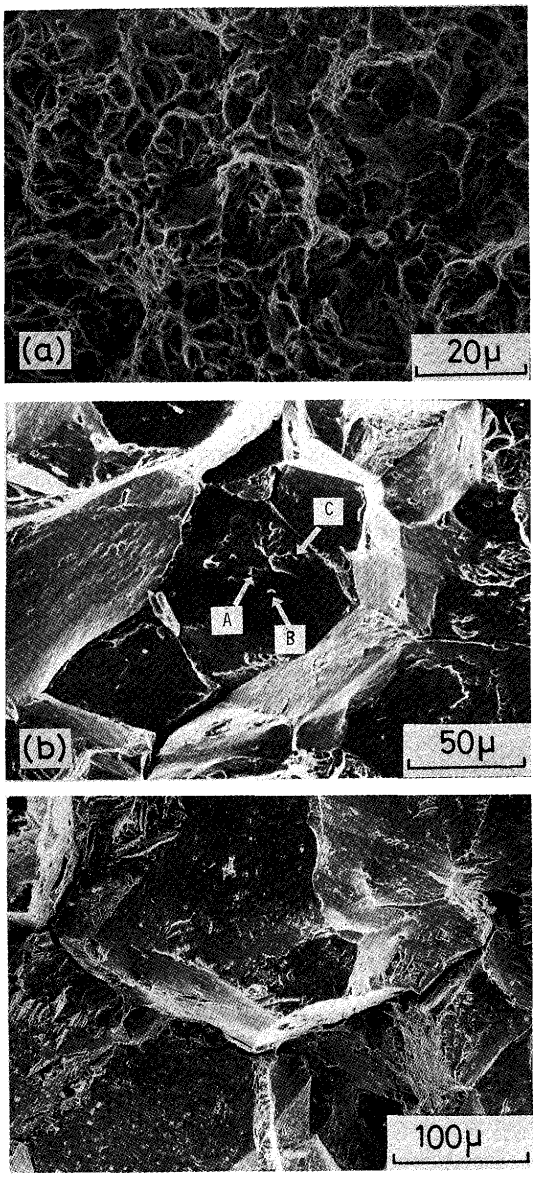

Fig. 5 Relation between morphology of intergranular fracture and austenization temperature for the specimen tempered at 300°C (A : Microvoid, B : Precipitates, C : Tear ridge). (a) : 850°C (b) : 1200°C and (c) : 1300°C

granular fracture surface shows considerably smooth surface, the subcracks along the grain boundary hardly generate. In the case of the specimen austenitized at 1200°C, the subcracks along the grain boundary hardly generates, but the microvoids, precipitates and tear ridges generate on the intergranular fracture surface respectively. Precipitates of round type were detected as Cr carbides by means of element analysis of X-ray energy dispersion method. In the case of the specimen austenitized at 1300°C, it is observed that the subcracks along the grain boundary generated and propagated inside the grain, and the patches[7] are present on the surface of grain boundary. Consequently, the increases of the austenitization tempera-

ture and grain size is related to the increase of the amount of tear ridges due to plastic deformation, and subcracks on the surface of the intergranular fracture.

Generally, it has been reported that the impurities such as sulfur, phospholus so on segregate to the grain boudary during austenitizing, and the amount of segregation decreases with increasing the austenitization temperature by means of Auger electron spectroscopy[5) 7)]. Consequently, that the amount of the tear ridge on the surface of intergranular fracture increases with increasing the austenitization temperature corresponds with the segregation phenomena of the elements mentioned, and the precipitation phenomena of the plate-like carbides precipitated along the austenite grain boundary. Namely, the grain boundary sulfides and carbides formed during austenitization and tempering treatment respectively may provide barriers for slip and then nucreate intergranular cracks.

3.2 Relation between tempered martensite embrittlement and hydrogen embrittlement

In order to inverstigate the relation between tempered martensite embrittlement and hydrogen embrittlement, the specimens were heated at 850°C for 15 sec, oil quenched, and then tempered at each temperature from 150°C to 600°C. The heat treated specimens were cathodically charged and pulled out.

Figure 6 shows the mechanical properties prior hydrogen charging, for various tempering treatments after

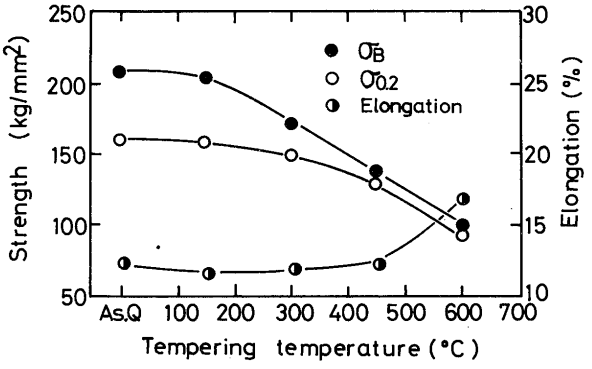

Fig. 6 Relation between mechanical properties and tempering temperature.

solution treatment at 850°C. The increase of the tempering temperature causes the decrease of the tensile strength and increase of the elongation, because of the decrease of the quench strain and precipitation of the carbides by tempering treatment. **Figure 7** shows the relation between tempering temperature and the susceptibility to hydrogen embrittlement.

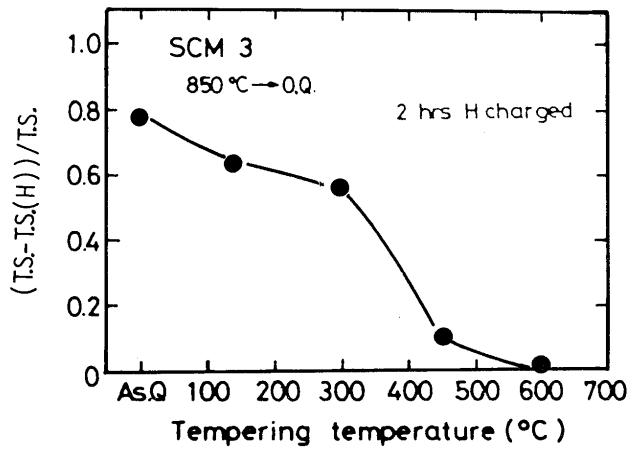

Fig. 7 Relation between susceptibility to hydrogen embrittlement and tempering temperature.

The index for susceptibility to hydrogen embrittlement (H) was evaluated as follows.

$$H = \{(\text{Tensile strength of uncharged specimen}) - (\text{Tensile strength of charged specimen})\} / (\text{Tensile strength of uncharged specimen})$$

The increase of the index means the increase of the susceptibility to hydrogen embrittlement. In the case of as-quenched specimen, the index of the susceptibility to hydrogen embrittlement shows maximum value, and it means that it is most susceptible to hydrogen embrittlement in the specimen tested. The susceptibility to hydrogen embrittlement decreases with increasing the tempering temperature. For 450°C and 600°C tempering temperature, the tensile strength by hydrogenation is equal to the strength of uncharged specimen, and it means that the susceptibility to hydrogen embrittlement is very low.

Generally, the hydrogen embrittlement has hardly affected to the tensile strength, but affected to the elongation and reduction in area, for pure irons and low carbon steels.

In the steel used in this investigation has 0.36% carbon and the tensile strength of 100 kg/mm², the hydrogenation to the specimen causes the decrease of the tensile strength as shown in Fig. 7. This results are also reported by Thompson et al[8)]. Especially, hydrogen charged tensile specimens did not exhibit yielding as loads at fracture were below those required to cause yielding in the uncharged condition. That means that the interaction of the slight plastic deformation below 0.2% proof stress and hydrogen in the matrix causes the hydrogen embrittlement.

3.3 Relation between fracture morphology of hydrogen embrittlement and tempering temperature

In order to investigate the relation between fracture morphology and hydrogen embrittlement, the fracture surfaces obtained were observed up to 2 mm inside the specimen from the surface. And then the relation between the intergranular fracture percentage and the tempering temperature is shown in **Fig. 8.**

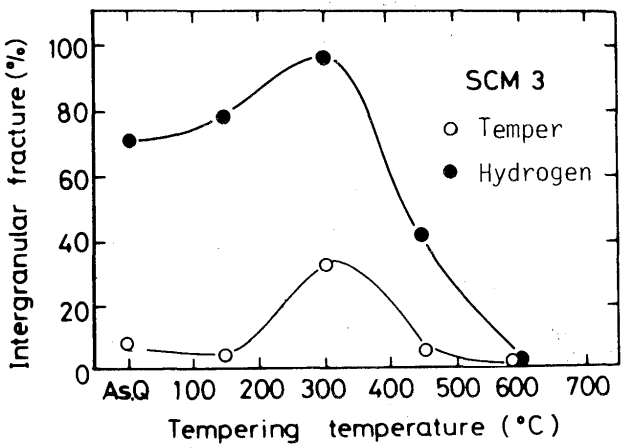

Fig. 8 Relation between percentage of intergranular fracture due to tempered embrittlement and hydrogen embrittlement, and tempering temperature.

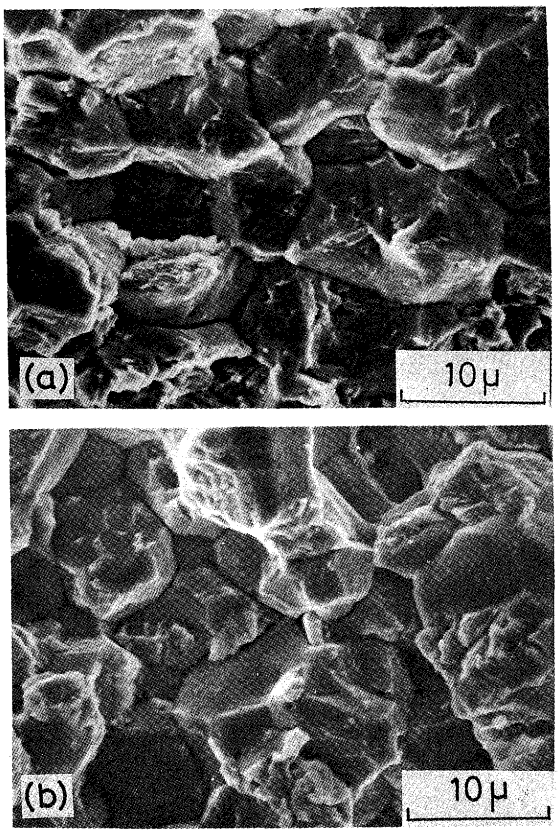

Fig. 9 Morphology of intergranular fracture due to hydrogen embrittlement.
(a) As-quenched. (b) Tempered at 300°C.

Because of the cathodic charging, the hydrogen concentration near the specimen surface is high, so that the fracture morphology showed hydrogen embrittlement, but the concentration is very low in the center of the specimen, so that the fracture morphology showed dimple pattern. In the Fig. 8, the results of the impact value is also added as the data for uncharged and tempered specimen. In the case of uncharged specimen, the intergranular fracture percentages of 30% is shown at the 300°C tempering, but, in the case of hydrogen charged specimen, the percentage is 100%. Both as-quenched specimen and the specimen tempered at 150°C show the high percentage of intergranular fracture. But for the specimen tempered at 600°C, the intergranular fracture hardly occurs.

Figure 9 indicates the change in the fracture morphology as both the as-quenched specimen and the specimen tempered at 300°C were oil-quenched after the austenitization at 850°C. For as-quenched specimen, the many tear ridges occur on the surface of intergranular fracture, and subcracks along the prior austenite grain boundary are also observed. This phenomena is different from the fracture surface of the tempered martensite embrittlement of uncharged specimen shown in Fig. 5.

Consequently, the fracture morphologies shown in Fig. 9 seems to be the characteristic morphology of hydrogen embrittlement. The other way, for the hydrogen charged specimen tempered at 300°C, the fracture surface was considerably smooth and was caused the plastic deformation. The intergranular fracture involved the plastic deformation and subcracks along the prior austenite grain boundary were hardly observed for the tempered martensite embrittlement of uncharged specimen. Consequently, the dimple fracture area due to tempered embrittlement treatment seems to have been changed to the intergranular fracture included more plastic deformation.

The smooth surface of intergranular fracture is similar to that of tempered martensite embrittlement, this surface cannot be distinguish whether the surface is due to hydrogen embrittlement or not. But the intergranular fracture of smooth surface seems to have caused along the interface of plate-like carbides and the matrix, and the fracture morphology seems to be caused by the interaction of the carbides and hydrogen in the matrix.

Figure 10 shows the morphologies of cleavage fracture and hydrogen embrittlement fracture. In the case of as-quenched specimens, the cleavage fracture for uncharged specimen consists of the fracture unit facet correlated to a lot of martensite lath, the unit facet size is large. For hydrogen embrittlement of as-quenched specimen, the

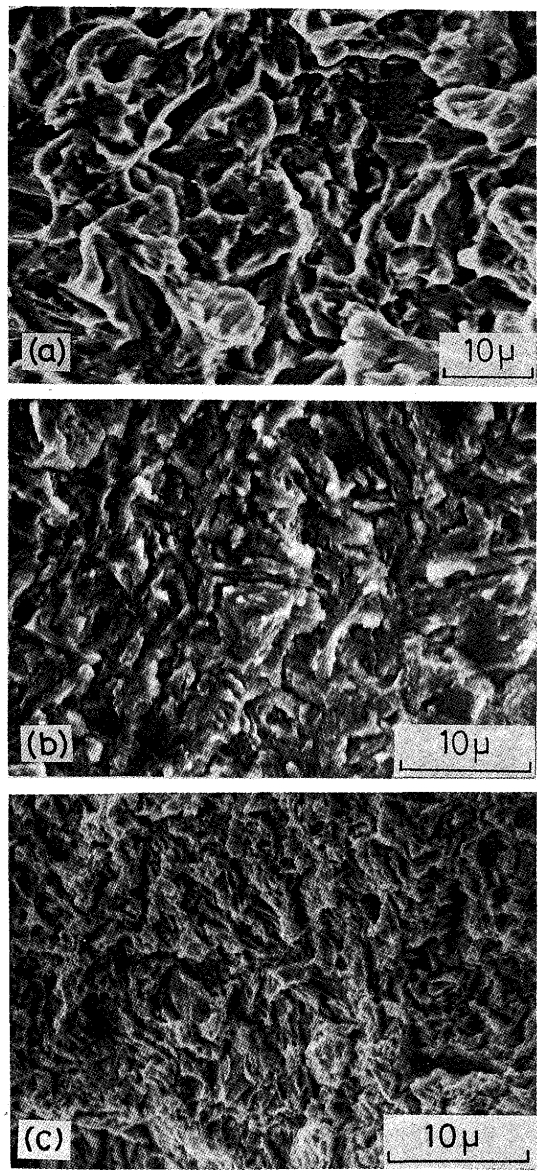

Fig. 10 Morphologies of cleavage fracture and hydrogen embrittlement fracture.
(a) Cleavage fracture of as-quenched specimen.
(b) Quasi-cleavage fracture due to hydrogen embrittlement for as-quenched specimen.
(c) Quasi-cleavage fracture due to hydrogen embrittlement for the specimen tempered at 600°C

quasicleavage fracture corresponds to the shape of martensite lath, the fracture unit facet size is small. Furthermore, the interface of the unit fracture facet each shows heavy tear ridge for the cleavage fracture.

For quasicleavage fracture due to hydrogen, the fracture morphology corresponds to the distribution of martensite lath, the martensite laths were caused considerably plastic deformation, and subcracks at the interface of the laths occurs. The fracture morphology is similar to that of high strength steel previously mentioned[1) 2)]. And the fracture morphology seems to be the characteristic morphology due to hydrogen embrittlement (QC_{HE}).

For the charged specimen tempered at 600°C, the fracture morphology shows quasi-cleavage fracture with many microvoids, because of the precipitation of the carbides as shown in Fig. 10. However, micro dimple fracture is observed at the inner area of the martensite lath, because that the hydrogen segregates at the microvoids generated at the interface of spheroidal carbides and the matrix, so that hydrogen concentration in the matrix may become lower.

4. Conclusions

An investigation has been made of the fracture morphologies of hydrogen embrittlement and tempered martensite embrittlement by means of fractography. The results obtained in this investigation are summarized as follows.

1) The susceptibility to hydrogen embrittlement is highest for the as-quenched specimen, and the susceptibility decreases with increasing the tempering temperature.
2) The intergranular fracture percentage due to hydrogen embrittlement shows near 100% value for the specimen caused the tempered martensite embrittlement at 300°C. The intergranular fracture due to the hydrogen embrittlement hardly occurs for 450°C and 600°C temper. The susceptibility to hydrogen embrittlement is considerably high up to the 300°C tempering temperature.
3) Concerning the intergranular fracture morphology, the tear ridges generated on the intergranular fracture surface due to only tempered martensite embrittlement increases with increasing the austenitization embrittlement. For the intergranular fracture due to hydrogen embrittlement, the tear ridges and subcracks on the surface occur more than that of tempered martensite embrittlement of uncharged specimen.
4) The transgranular fracture due to hydrogen embrittlement has characterized by the quasicleavage fracture due to hydrogen embrittlement, and subcracks along the lath boundary, and different from that of cleavage fracture occured at low temperature.

Reference

1) F. Terasaki and F. Nakasato, Report of Delayed failure meeting, Iron Steel Inst. of Japan, (1975). (in Japanese).
2) Y. Kikuta, T. Araki and T. Kuroda, Analysis of Fracture Morphology of Hydrogen-Assisted Cracking in Steel and Its Welds, ASTM STP 645, 107, (1978).

3) F. Nakasato and F. Terasaki, Delayed Failure Characteristics of Ultra High Strength Steels, J. Iron, Steel Inst. of Japan, 61, 841, (1975). (in Japanese)

4) S. Fukui, J. Iron Steel Inst. of Japan, 55, 151, (1969). (in Japanese)

5) C.L. Briant and S.K. Banerji, Tempered Martensite Embrittlement in Phosphorus Doped Steels, Met. Trans. 10A, 1729, (1979).

6) J.P. Materkowski and G. Krauss, Tempered Martensite Embrittlement in SAE 4340 Steel, Met. Trans. 10A, 1645, (1979).

7) C.L. Briant and S.K. Banerji, Tempered Martensite Embrittlement and Intergranular Fracture in an Ultra-High Strength Sulfur Doped Steel, Met. Trans. 12A, 309, (1981).

8) J.E. Costa and A.W. Thompson, Effect of Hydrogen on Fracture Behavior of a Quenched and Tempered Medium-Carbon Steel, Met. Trans. 12A, 761, (1981).